# Image Cover Sheet

| CLASSIFICATION | SYSTEM NUMBER | 152436 |
|---|---|---|
| UNCLASSIFIED | | |

**TITLE**

ALGERBRAIC APPROXIMATIONS TO EXTINCTION FROM RANDOMLY ORIENTED CIRCULAR AND ELLIPTICAL CYLINDERS

**System Number:**

**Patron Number:**

**Requester:**

**Notes:**

DSIS Use only:

Deliver to:

Défense National
nationale Defence

**UNCLASSIFIED**

DEFENCE RESEARCH ESTABLISHMENT
CENTRE DE RECHERCHES POUR LA DÉFENSE
VALCARTIER, QUÉBEC

### DREV - R - 9425

Unlimited Distribution/Distribution illimitée

## ALGEBRAIC APPROXIMATIONS TO EXTINCTION FROM RANDOMLY ORIENTED CIRCULAR AND ELLIPTICAL CYLINDERS

by

G.R. Fournier and B.T.N. Evans

June/juin 1995

Canada

**SANS CLASSIFICATION**

**UNCLASSIFIED**

DEFENCE RESEARCH ESTABLISHMENT
CENTRE DE RECHERCHES POUR LA DÉFENSE
VALCARTIER, QUÉBEC

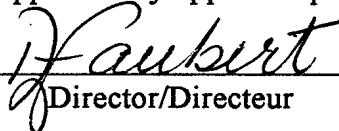DREV - R - 9425

Unlimited Distribution/Distribution illimitée

## ALGEBRAIC APPROXIMATIONS TO EXTINCTION FROM RANDOMLY ORIENTED CIRCULAR AND ELLIPTICAL CYLINDERS
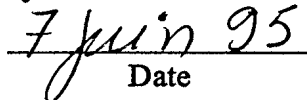
by

G.R. Fournier and B.T.N. Evans

June/juin 1995

Approved by/approuvé par

*Faubert*

Director/Directeur

*7 juin 95*

Date

i

## ABSTRACT

Analytic approximations to the extinction efficiency, $Q_{ext}$, for oriented and randomly oriented circular infinite cylinders based on anomalous diffraction are given. The results are compared with the exact code. These results are further generalized to randomly oriented elliptical cylinders. Using the formulae, $Q_{ext}$ can be evaluated over $10^4$ times faster than with the exact code. This approximation is valid for complex refractive indices $m = n - ik$, where $1 \leq n \leq \infty$ and $0 \leq k \leq 3$, aspect ratios from 1 to 4 and modest to large particle sizes. The accuracy and limitations of these formulae are discussed.

## RÉSUMÉ

Nous présentons une approximation analytique de l'efficacité d'extinction $Q_{ext}$ pour des cylindres infinis à orientation fixe et aléatoire. Cette approximation est comparée au calcul exact. Ces résultats sont étendus aux cylindres elliptiques orientés aléatoirement. Grâce à cette formule, $Q_{ext}$ peut être évalué $10^4$ fois plus vite que par les méthodes antérieures. Nous avons vérifié cette formule pour des indices de réfraction complexes $m = n - ik$, où $1 \leq n \leq \infty$ et $0 \leq k \leq 3$, pour des aspects de 1 à 4 et pour des particules de taille moyenne à grosse. Ces formules sont basées sur la théorie de la diffraction anomalique. L'exactitude de ces formules ainsi que leurs limites sont discutées.

UNCLASSIFIED
iii

## TABLE OF CONTENTS

FIGURES 1 to 16

v

# EXECUTIVE SUMMARY

The present and future electro-optic capabilities of fire control systems require or will require full spectrum obscurants as an effective countermeasure. It is well known that spherical particles, such as those created in phosphorous based obscurants, can obscure efficiently only in the visible region of the spectrum. In the near and far infrared as well as the microwave region of the spectrum, the use of high aspect, highly conductive cylindrical particles is mandatory. For example, carbon fibers or iron whiskers are being considered. Furthermore, reduced visibilities due to elongated ice crystals in cirrus clouds or cylindrically shaped hydrosols will be modelled in future realistic military simulations.

The objective of this work is to reduce significantly the computational burden in calculating the extinction from randomly oriented cylindrical (ROC) particles that are very long in comparison with the considered wavelength. This allows for the exploration and rapid computation of the effects of varying size distributions and material properties of the ROC particles on the performance of obscurants and on electromagnetic propagation in general.

To date, the estimation of reduced visibilities due to aerosols or hydrosols in military simulation has been extremely crude or non-existent. This is in part due to the complex and computationally inefficient codes required to estimate the extinction. This work overcomes both of these restrictions. For instance, a factor greater than ten thousand in computational speed has been achieved with minimal loss in accuracy. Furthermore, far less technical knowledge of numerical computation is required.

The long-term goal of this work is to alleviate the remaining constraints in the theoretical consideration of non-spherical aerosols and obscurants of both natural and artificial origin. This will not only aid in finding better obscurants and allowing more accurate and efficient simulations, but also in the possible identification and remote classification of such aerosols.

1

## 1.0 INTRODUCTION

The immediate objective of this work is to reduce significantly the computational burden in calculating the extinction from cylindrical particles. This allows for the exploration of the effects of cylindrical particles on the performance of electro-optical and millimeter wave systems in obscurants, ice clouds and hydrosols.

The current calculation with randomly oriented infinite cylinders can require large computation times, especially for polydispersions, larger particle sizes and refractive indices.

We have previously presented (Ref. 1) an analytic approximation to $Q_{ext}$ for randomly oriented spheroids. This work applies to particles with $n > 1$ and $k > 0$ for arbitrary sizes and aspect ratios. The basic approach was to orthogonalize as much as possible the scattering physics into well-defined regimes. The large particle regime was successfully modelled by anomalous diffraction and edge (Fock) terms. Here we will take the same basic approach but applied to randomly oriented cylinders instead.

The report is organized as follows: Chapter 2.0 develops the extinction formula. Chapter 3.0 contains comparisons of this approximation to the exact code from IPHASE (Ref. 2), Chapter 4.0 extends the anomalous diffraction approach and explores the ramifications, and Chapter 5.0 develops and discusses approximations to randomly oriented elliptical cylinder extinction. The final chapter, Chapter 6.0, gives the conclusions and limitations.

UNCLASSIFIED
2

This work was performed at DREV between October 1993 and November 1994 under PSC 32A, EO/IR Protection of Land Vehicles.

## 2.0   DEVELOPMENT OF THE EXTINCTION FORMULA

The physics and the structure of the extinction formula for randomly oriented cylinders will be developed in this chapter. Only medium to large size parameters will be considered. Hence these formulae will not apply in the small particle or Rayleigh region.

### 2.1   Anomalous Diffraction Term

The anomalous diffraction approach was first discussed by Van de Hulst (Ref. 3) for spheres. Furthermore, it was extensively developed for oriented infinite cylinders by Stephens (Ref. 4).

The anomalous diffraction formula is derived by assuming that the incident plane wave is not significantly skewed in passing through the scattering object and that, to first order, the effect of the scatterer is to delay locally the phase of the wave and attenuate its amplitude (Ref. 3). The strict limit of validity of the formula is therefore the region where $(n-1) << 1$. The cylinder is in effect treated as a slit normal to the incident wave possessing a spatially dependent phase and amplitude. The Fraunhofer pattern at infinity

is then derived and $Q_{ext}$ evaluated from the standard relations. For a cylinder with its axis oriented at an angle $\theta$ with respect to the direction of the incident radiation, this procedure leads immediately to the following formula (Ref. 4) :

$$Q_{ad} = \pi \text{Re}[\text{H}_1(\omega) + i\text{J}_1(\omega)] \qquad [1]$$

where $\omega$ is given by

$$\omega = 2(m-1)x/\sin\theta, \qquad [2]$$

the complex refractive index is $m = n - ik$ and $x$ is the size parameter. In the above $\text{H}_1$ and $\text{J}_1$ are the first order Struve and Bessel functions, respectively. These are well defined in Ref. 5. Clearly, when the index is real only the first term in [1] appears.

For random orientation, the angle averaging gives

$$\overline{Q}_{ad} = \frac{\int_0^{\pi/2} Q_{ad} \sin^2\theta \, d\theta}{\int_0^{\pi/2} \sin^2\theta \, d\theta} \qquad [3]$$

$$= 4\text{Re}\left[\int_0^{\pi/2} \text{H}_1(\omega) \sin^2\theta \, d\theta + i\int_0^{\pi/2} \text{J}_1(\omega) \sin^2\theta \, d\theta\right]. \qquad [4]$$

The first term in [4] can be analytically integrated as follows:

$$4\int_0^{\pi/2} \text{H}_1(\rho/\sin\theta) \sin^2\theta \, d\theta = 2\int_1^{\infty} \frac{\text{H}_1(\rho\sqrt{z}) \, dz}{z^2\sqrt{z-1}} \qquad [5]$$

by using the simple transform $z = 1/\sin^2\theta$. This integral appears as a special case of equation 2.7.4.6 in Ref. 8. We will use a more general approach initially for later purposes. We will solve it by using a general hypergeometric form of the above Weyl type integral.

4

From Ref. 6, p. 417, formula 20.5 (2),

$$\int_1^\infty x^{-\eta}(x-1)^{\sigma-1} G_{pq}^{mn}\left(ax \middle| \begin{array}{c} \alpha_p \\ \beta_q \end{array}\right) dx = \Gamma(\sigma) G_{p+1,q+1}^{m+1,n}\left(a \middle| \begin{array}{c} \alpha_p, \eta \\ \eta-\sigma, \beta_q \end{array}\right) \qquad [6]$$

where $G_{pq}^{mn}$ is the Meijer G-function. The Struve function is represented by the following

G-function (Ref. 7):

$$\mathbf{H}_1(x) = G_{1,3}^{1,1}\left(\frac{x^2}{4} \middle| \begin{array}{c} 1 \\ 1, \frac{1}{2}, -\frac{1}{2} \end{array}\right). \qquad [7]$$

Using [7] and [6] in [5] we get

$$\begin{aligned}
2\int_1^\infty \frac{\mathbf{H}_1(\rho\sqrt{z})\,dz}{z^2\sqrt{z-1}} &= 2\int_1^\infty z^{-2}(z-1)^{-1/2} G_{1,3}^{1,1}\left(\frac{\rho^2 z}{4}\middle| \begin{array}{c} 1 \\ 1,\frac{1}{2},-\frac{1}{2}\end{array}\right) dz \\
&= 2\Gamma(\tfrac{1}{2}) G_{2,4}^{2,1}\left(\frac{\rho^2}{4}\middle| \begin{array}{c} 1,2 \\ \frac{3}{2},1,\frac{1}{2},-\frac{1}{2}\end{array}\right).
\end{aligned} \qquad [8]$$

Following Ref. 7, p. 230 6.5 (1) the above G-function can be reduced, giving

$$2\Gamma(\tfrac{1}{2}) G_{2,4}^{2,1}\left(\frac{\rho^2}{4}\middle| \begin{array}{c} 1,2 \\ \frac{3}{2},1,\frac{1}{2},-\frac{1}{2}\end{array}\right) = 2\rho^2\left\{\frac{2}{3} - \frac{\rho\pi}{16}\, {}_1F_2\left[\begin{array}{c} \frac{1}{2} \\ 2,3\end{array}\middle| \frac{-\rho^2}{4}\right]\right\}. \qquad [9]$$

This equation can be directly obtained by equation 2.7.4.6 of Ref. 8 as mentioned above.

The $_1F_2$ in [9] can be further simplified by expressing it in terms of Bessel functions of the

first kind. Formulae to accomplish this can be found (Ref. 8), giving finally

$$2\int_1^\infty \frac{\mathbf{H}_1(\rho\sqrt{z})\,dz}{z^2\sqrt{z-1}} = \frac{4}{3}\rho^2\left\{1 - \frac{\rho\pi}{4}\left[\mathbf{J}_0^2(\rho/2) - \frac{2}{\rho}\mathbf{J}_0(\rho/2)\mathbf{J}_1(\rho/2) + \left(1-\frac{2}{\rho^2}\right)\mathbf{J}_1^2(\rho/2)\right]\right\}. \qquad [10]$$

The above equation is the full solution to $Q_{ad}$ for real indices. It is remarkably simple and

is readily computable.

The second term in [4] is treated as follows:

$$4i\int_0^{\pi/2} \mathbf{J}_1(\rho/\sin\theta)\sin^2\theta\,d\theta = 2i\int_1^\infty \frac{\mathbf{J}_1(\rho\sqrt{z})\,dz}{z^2\sqrt{z-1}}. \qquad [11]$$

[12]

This integral in not explicitly in the integral tables, so we will use [6] and the G-function representation of $J_1$:

$$J_1(x) = G_{0,2}^{1,0}\left(\frac{x^2}{4}\middle|\begin{array}{c} - \\ \frac{1}{2}, -\frac{1}{2}\end{array}\right).$$
[13]

This gives

$$\begin{aligned}
2i\int_1^\infty \frac{J_1(\rho\sqrt{z})\,dz}{z^2\sqrt{z-1}} &= 2i\int_1^\infty z^{-2}(z-1)^{-1/2}G_{0,2}^{1,0}\left(\frac{\rho^2 z}{4}\middle|\begin{array}{c} - \\ \frac{1}{2}, -\frac{1}{2}\end{array}\right)\,dz \\
&= 2i\Gamma(\tfrac{1}{2})\,G_{1,3}^{2,0}\left(\frac{\rho^2}{4}\middle|\begin{array}{c} 2 \\ \frac{3}{2},\frac{1}{2},-\frac{1}{2}\end{array}\right).
\end{aligned}$$
[14]

This G-function can be shown to be of the logarithmic type, which means that no finite expression in terms of hypergeometric functions can be obtained. However, it can be formally expressed as an infinite series giving for [14] the following:

$$2i\Gamma(\tfrac{1}{2})\,G_{1,3}^{2,0}\left(\frac{\rho^2}{4}\middle|\begin{array}{c} 2 \\ \frac{3}{2},\frac{1}{2},-\frac{1}{2}\end{array}\right) = \frac{i\rho}{4}\left\{4 + \frac{\rho^2}{4}\ln\frac{\rho^2}{4}\,_1F_2\left[\begin{array}{c}\frac{1}{2}\\2,3\end{array}\middle| -\frac{\rho^2}{4}\right] + \right.$$
$$\left. \sum_{k=0}^\infty \left(-\frac{\rho^2}{4}\right)^{k+1}\frac{(1/2)_k}{(2)_k(3)_k k!}\left[3\psi(k+1) - \psi(k-\frac{1}{2}) + \frac{2}{1-2k} + \frac{2}{1+k} + \frac{1}{2+k}\right]\right\}.$$
[15]

In the above, $\psi(z)$ is the digamma function and $(a)_k$ is the Pochhammer symbol (Ref. 5). Due to the slow convergence of the sum in [15], for even modestly large $\rho$, it is not of great computational value. Therefore, another simpler approximation is required.

We go back to the physical level. When there is no absorption, there is constructive and destructive interference. This produces the familiar oscillations in $Q_{ext}$. This is well described by [10]. Absorption affects the interference spatially by reducing the amplitude of the partial waves inside the particle. This has the effect of damping the magnitude of

6

the oscillations in $Q_{ext}$. For very large absorptions the particle is opaque, no waves are transmitted and hence, by Babinet's principle, $Q_{ext} = 2$. To first order we will neglect the spatial dependence that absorption has on the interference. We will do this by averaging the absorption length $2ky/\sin\theta$ spatially and over angles. Here $y$ is a cord length through the cylinder. The angular average is given by

$$\frac{\int_0^{\pi/2} \left(\frac{2ky}{\sin\theta}\right) \sin^2\theta \, d\theta}{\int_0^{\pi/2} \sin^2\theta \, d\theta} = \frac{8ky}{\pi}. \qquad [16]$$

Then doing the spatial averaging to get the final averaged absorption length $\lambda$:

$$\begin{aligned}
\lambda &= \frac{2\int_0^x \frac{8ky}{\pi} dz}{2\int_0^x dz} \\
&= \frac{8k}{\pi x} \int_0^x \sqrt{x^2 - z^2} \, dz \\
&= 2kx. \qquad [17]
\end{aligned}$$

This simple average gives $e^{-\lambda}$ as the approximate damping factor. Note that averaging $e^{-2ky/\sin\theta}$ produces another logarithmic G-function of similar complexity as [15].

The oscillating terms can be isolated from $Q_{ad}$ (for real $m$) by subtracting from it the constant 'Babinet' term, which is 2. These can then be damped by $e^{-\lambda}$ and then the 'Babinet' term added back. Thus the approximation to $Q_{ad}$ including absorption becomes

$$Q_{ad} \approx 2 + e^{-2kx} \left(\frac{4}{3}\rho^2 \left\{ 1 - \frac{\rho\pi}{4}\left[ J_0^2(\rho/2) - \frac{2}{\rho} J_0(\rho/2) J_1(\rho/2) + \left(1 - \frac{2}{\rho^2}\right) J_1^2(\rho/2) \right] \right\} - 2 \right)$$

$$[18]$$

where $\rho = 2(n-1)x$. Note that $\rho$ is now always real.

7

## 2.2    Edge Effects

For a particle whose typical size is much larger than the wavelength, the edge cannot be treated as sharp and the effect of the curvature of the object must be included. Jones (Ref. 9) has shown how to estimate these edge effects for convex bodies. As he clearly explains, near a glancing point, the body will behave approximately like a cylinder with its axis perpendicular to the surface normal (at the glancing point) and the direction of propagation of the incident wave. The scattering and absorption from all such cylindrical sections can be integrated around the projection of the penumbral curve to give the total contribution of the edge effects to the extinction cross section. The projection is onto the plane normal to the incident ray direction. The energy scattered per unit length of the cylinder by region on its surface around the glancing point is proportional to $c_{TE}R^{1/3}$ for the TE mode and $c_{TM}R^{1/3}$ for the TM mode, where $R$ is the radius of curvature of the cylinder. The constants $c_{TE}$ and $c_{TM}$ are the first order Fock terms. It can be shown that, for convex bodies, randomly oriented or illuminated by a randomly polarized beam, $(c_{TE} + c_{TM})/2 = c_e$, where $c_e$ is a universal function of refractive index. Following Jones, the edge contribution to the extinction efficiency of the body is

$$Q_{edge} = \frac{c_e}{S} \int_P R^{1/3}\, ds \qquad [19]$$

where $S$ is the projected area of the body on a plane normal to the direction of propagation of the incident wave and $s$ is the arc length along the projection of the shadow boundary $P$ on that same plane.

From the basic geometry of the cylinder, the terms in [19] become

$$S = 2xl \sin \theta, \qquad ds = 2 \sin \theta \, dl, \qquad R = \frac{x}{\sin^2 \theta} \qquad [20]$$

where $l$ is a unit length along the cylinder axis. Thus $Q_{edge}$ becomes

$$Q_{edge} = \frac{c_e}{(x \sin \theta)^{2/3}}. \qquad [21]$$

The angle averaging of [21] to obtain $\overline{Q}_{edge}$ is straightforward:

$$\overline{Q}_{edge} = \frac{\int_0^{\pi/2} Q_{edge} S \sin \theta \, d\theta}{\int_0^{\pi/2} S \sin \theta \, d\theta} = \frac{2}{\sqrt{\pi}} \frac{\Gamma(7/6)}{\Gamma(5/3)} \frac{c_e}{x^{2/3}} \approx \frac{1.159595 c_e}{x^{2/3}}. \qquad [22]$$

This universal function $c_e$ is not known. Since $c_e$ is independent of shape, this could be accomplished by studying the sphere alone. This however, probably produces a function that is much too complex to be included in a simple formula. We therefore use the value for optically soft particles $c_e^{soft} = c_0 = 0.996130$, (Refs. 11-12). and (Ref. 12). An added complication to $\overline{Q}_{edge}$ arises, however, when we consider cylinders with small complex phases $\psi x$. This means that, for randomly oriented cylinders, $|\psi|x = 2|m-1|x << 1$. This occurs since what we have been calling an edge effect is in fact the field distortion around the boundaries of the particle, and hence its behaviour for small phase is different from that for large phases. A simple semi-empirical model of the above two behaviours is:

$$\overline{Q}_{edge} = \frac{1.159595 c_0}{x^{2/3} + x_{crit}}$$

$$x_{crit} = \frac{\rho_{max}}{2|\psi|}. \qquad [23]$$

Here $\rho_{max}$ is the value of the phase at the first maximum of $Q_{ext}$ for real indices. Thus $x_{crit}$ is the size parameter that is approximately midway between 0 and the first peak.

Hence [23] is designed to have the proper asymptotic behaviour for $x^{2/3} \gg x_{crit}$ and is just a constant for $x^{2/3} \ll x_{crit}$. For spheres, $\rho_{max} \approx 4$ and for randomly oriented infinite cylinders $\rho_{max} \approx \pi$. Thus [23] for randomly oriented infinite cylinders becomes

$$\overline{Q}_{edge} = \frac{1.159595c_0}{x^{2/3} + \pi/(4|m-1|)}. \qquad [24]$$

The large particle limit for the randomly oriented infinite cylinders becomes

$$Q_{ext} \rightarrow 2 + \overline{Q}_{edge}. \qquad [25]$$

We now wish to produce a term T which, when it multiplies [18], gives the same limit as [25] without diverging as the size parameter goes to zero. We found that (Ref. 10) an adequate expression for our purposes is

$$T = 2 - e^{-\overline{Q}_{edge}/2}. \qquad [26]$$

Other orderings of the angle averaging of the anomalous diffraction and edge term expressions and their products could have been done, but complex expressions such as [15] and worse occur (see Ref. 1).

10

## 2.3    Extinction Formula

From the formulae in the previous two sections the final formula for $Q_{ext}$ of randomly oriented infinite cylinders of medium to large size becomes

$$\left[2+e^{-2kx}\left(\tfrac{4}{3}\rho^2\left\{1-\tfrac{\rho\pi}{4}\left[J_0^2(\rho/2)-\tfrac{2}{\rho}J_0(\rho/2)J_1(\rho/2)+\left(1-\tfrac{2}{\rho^2}\right)J_1^2(\rho/2)\right]\right\}-2\right)\right]\left(2-e^{-\overline{Q}_{edge}/2}\right)$$

$$[27]$$

This result is valid for $n \geq 1$ and $k \geq 0$.

It is of interest to derive the large $\rho$ limit of [18] which is the backbone of [27] and thereby determining the peaks and valleys of the extinction curve. We do this by substituting Hankel's asymptotic expressions for the Bessel function equation 9.2.5 (Ref. 5). The result to order $1/\rho^2$ is

$$Q_{ad}^{cylinder} \asymp 2 - 4\frac{\cos\rho}{\rho} + \frac{3}{2}\left(\frac{1-4\sin\rho}{\rho^2}\right). \qquad [28]$$

This expression is important since it is similar to the anomalous diffraction expression derived by van de Hulst (Ref. 3) for spheres:

$$Q_{ad}^{sphere} = 2 - 4\frac{\sin\rho}{\rho} + 4\left(\frac{1-\cos\rho}{\rho^2}\right). \qquad [29]$$

Notice that they are nearly the same apart from an approximate phase shift of $\pi/2$ in $\rho$. This implies that the peaks and valleys of $Q_{ext}$ are also shifted in the randomly oriented cylinder case by approximately $\pi/2$. Indeed the nth peak is at about $2\pi(n-1/2)$ for cylinders

UNCLASSIFIED

11

versus $2\pi(n - 1/4)$ for spheres. Similarly, the valleys are at about $2\pi n$ for cylinders versus $2\pi(n + 1/4)$ for spheres.

## 3.0   RESULTS

The complete formula, as presented in the previous chapter, gives correct asymptotic behaviour for both large and small $|n - 1|$, $k \leq 1$ and $x \geq 1$. In studying the error behaviour of the approximation, the mid-ranges of $|m - 1|$ and $x$ are of greatest interest. In this chapter we will compare the analytic approximation with the exact randomly oriented cylinder code as implemented in IPHASE  (Ref. 2).

Figure 1 shows the comparison of $Q_{ext}$ versus $x$ for a refractive index of $n = 1.3$, close to that of ice in the visible. It is clear that the error decreases for large $x$. The largest errors are near and around the first two peaks. More of the scattering physics must be considered. All the peaks/valleys, while they are well modelled, are underestimated/overestimated. This occurs since anomalous diffraction assumes that the rays are not refracted by the particle and therefore overestimates the phase difference as a function of angle. In the next section, the anomalous diffraction formulation will be extended to account for this effect.

For small $k$ and large $n$ one can expect a significant contribution from surface waves. This effect is shown in Fig. 2 for an index of $m = 1.8 - 0\,i$. Unlike those for a sphere (Ref. 1), these resonant waves do not contribute as much and hence the present approximation does much better.
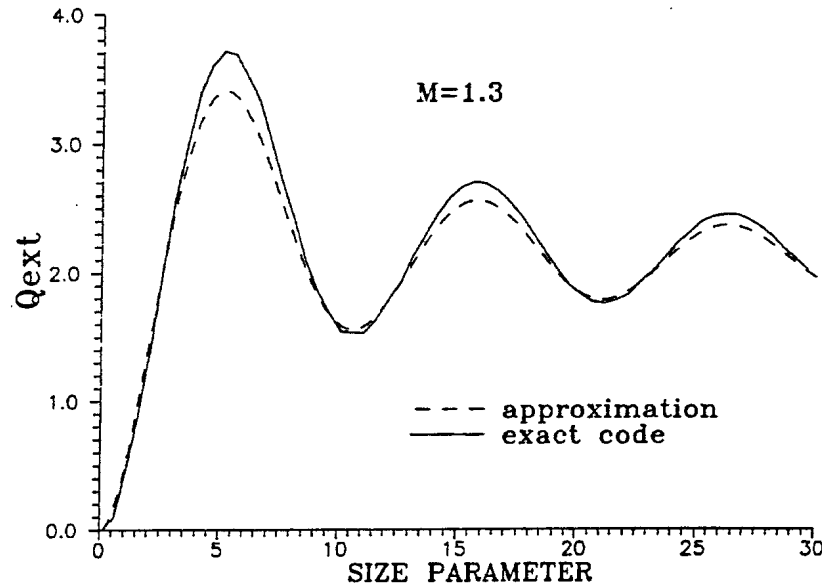
12



FIGURE 1 – Comparison between approximation and randomly oriented cylinder code for an index of 1.3. $Q_{ext}$ of ice in the visible.

For large $n$, body resonances can occur. These are sometimes called morphology dependent resonances (MDR). For spheres, these occur near $nx = l\pi$, where $l$ is a natural number. For cylinders, in any orientation, they occur at the first roots of the integer order Bessel functions. Hence, the MDR's occur when $J_l(nx) \approx 0$. For example the first MDR occurs when $nx \approx 2.40$.

Figure 3 shows an example of an incipient MDR on the first diffraction peak of $Q_{ext}$. Here, $m = 3 - 0\,i$. Note that, despite the significant perturbation in the transition region due to the MDR, the approximation is excellent.

The next two figures are for ice cylinders in the $3 - 5\,\mu$m and $8 - 12\,\mu$m regions, respectively. In Fig. 4 the diffraction peaks, as in the previous figures, are underestimated. Figure 5 is a case with large absorption and shows that the simple exponential damping
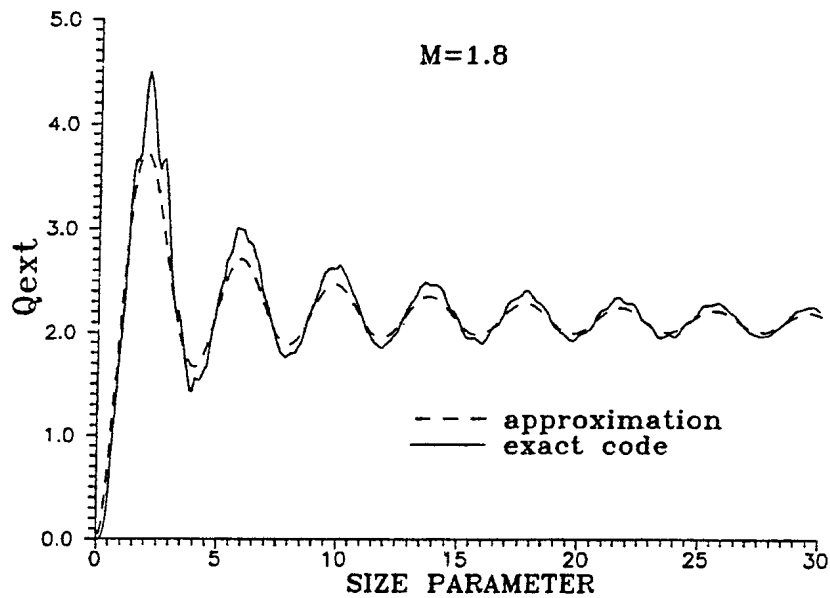
13



FIGURE 2 – Comparison between approximation and randomly oriented cylinder code for an index of 1.8 and an aspect ratio of 1; significant surface waves.
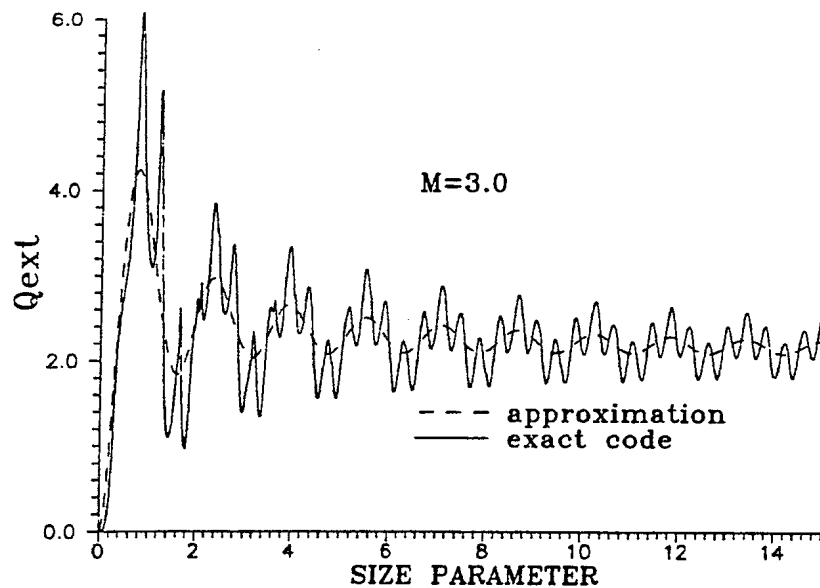


FIGURE 3 – Comparison between approximation and randomly oriented cylinder code for an index of $3 - 0\,i$; incipient MDR at $x \approx 0.8$.
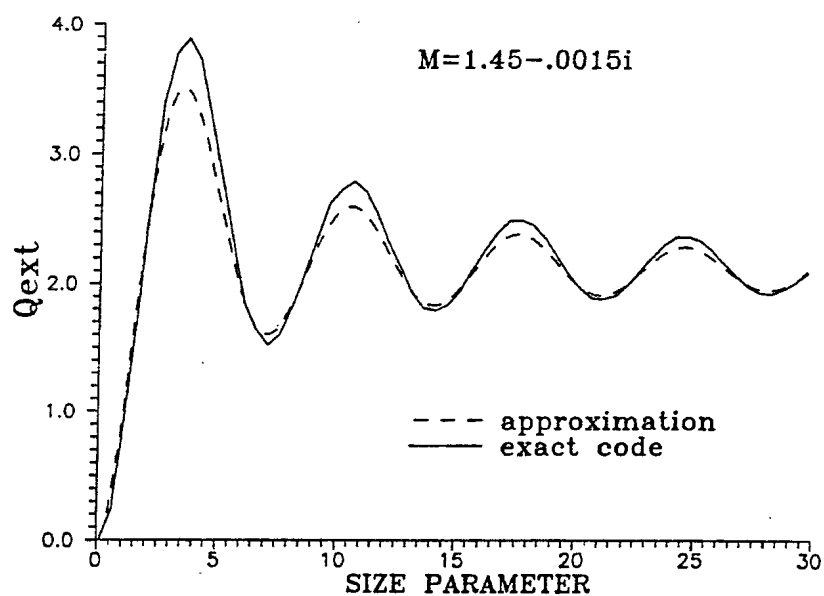
14



FIGURE 4 – Comparison between approximation and randomly oriented cylinder code for an index of $1.45 - 0.0015i$. $Q_{ext}$ of ice in the mid-infrared.
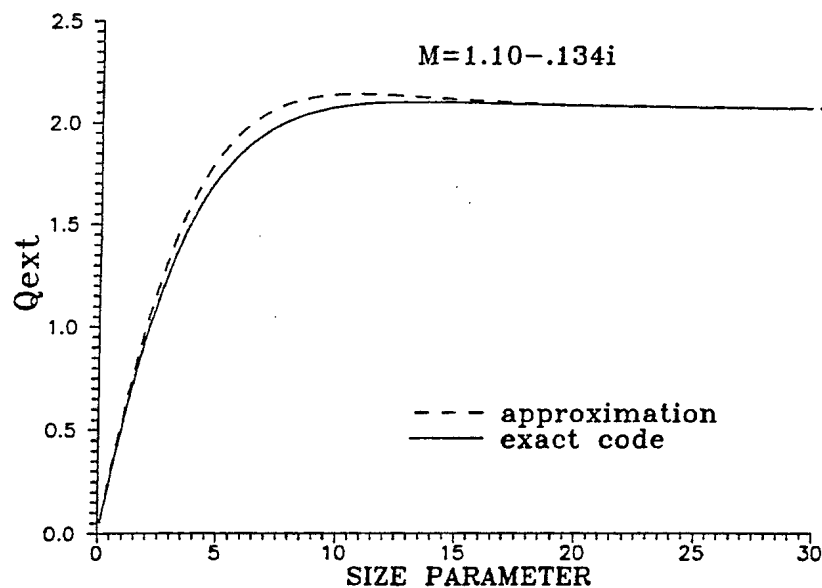


FIGURE 5 – Comparison between approximation and randomly oriented cylinder code for an index of $1.10 - 0.134i$. $Q_{ext}$ of ice in the far-infrared.

15

term $e^{-2kx}$, in [18], is quite successful in modelling the rise of the extinction.

Figure 6 represents the calculation for typical hydrosols. Many particles that are suspended in water have an absolute index of about 1.4. Thus the index to be considered in the scattering process is relative to water. Hence, in this example, $m \approx 1.4/1.33 \approx 1.05$. This is the region where anomalous diffraction applies and the excellent agreement with the exact results in Fig. 6 testifies to this.

The last two figures in this section are for carbon fibers in the ultraviolet to visible and $3 - 5\,\mu\text{m}$ regions. Figure 7 has even higher absorption than that of Fig. 5 but is still well modelled. As in all the above cases for $x < 1$ we do not expect very good agreement since there has been no attempt to model the Rayleigh region. In Fig. 8, the absorption is extremely high and is high enough for the particle to be reflective. The overestimate of $Q_{ext}$ for $x < 3$ is due to a breakdown of our model of the edge effect.

All our approximate $Q_{ext}$ diagrams in this chapter were produced at a rate of greater than $10^4$ times faster than by the exact code. The execution time for the approximation on an Intel i860 40 MHz coprocessor is about $70\,\mu\text{s}$ and is independent of particle size and index. This large speed up factor is essential if a complex computer model requires a large number of computations such as in a realistic military simulation.
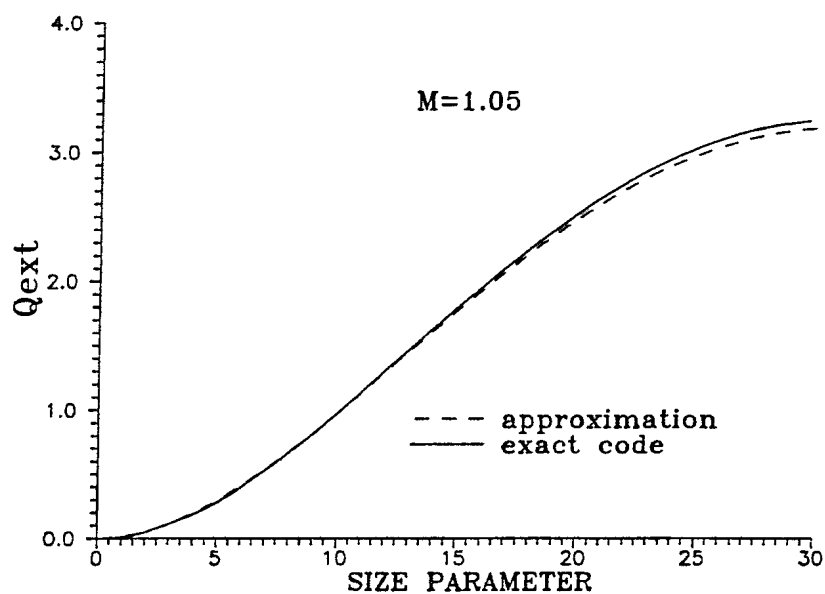
16



FIGURE 6 – Comparison between approximation and randomly oriented cylinder code for an index of 1.05. $Q_{ext}$ of hydrosols in the visible.
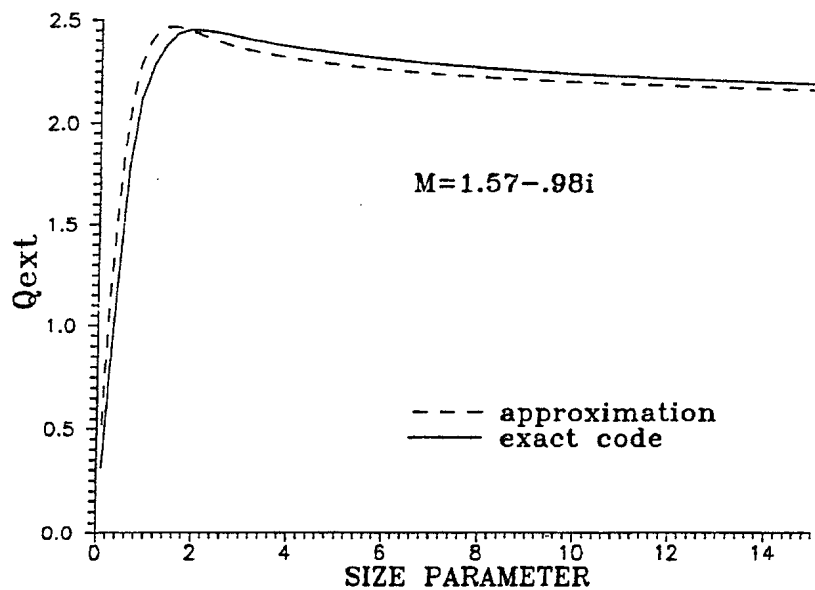


FIGURE 7 – Comparison between approximation and randomly oriented cylinder code for an index of $1.57 - .98\,i$. $Q_{ext}$ of carbon fibers in the ultraviolet to visible.
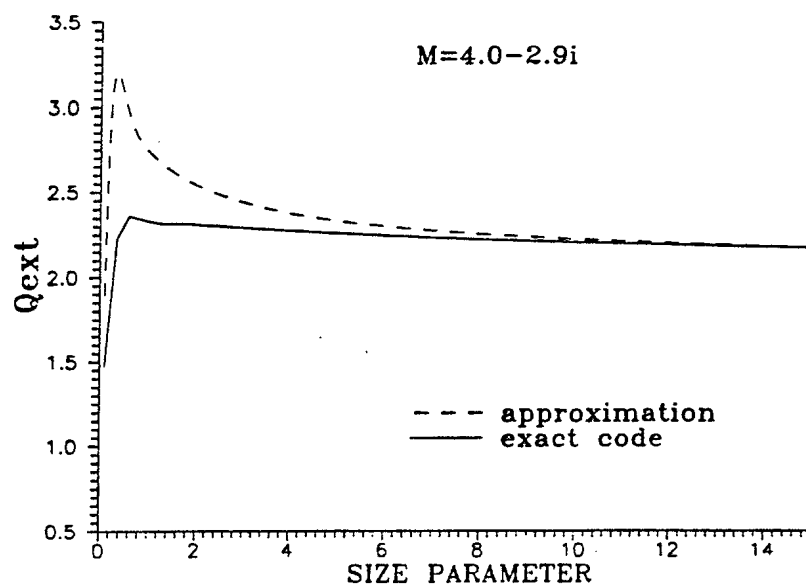
17



FIGURE 8 – Comparison between approximation and randomly oriented cylinder code for an index of $4-2.9\,i$. $Q_{ext}$ of carbon fibers in the mid-infrared.

## 4.0    EXTENDED ANOMALOUS DIFFRACTION

In the previous chapter it was pointed out that the standard anomalous diffraction underestimates/overestimates the peaks/valleys in the extinction curve since only undeviated rays are considered. In this chapter the extended anomalous formalism will be applied first to oriented infinite cylinders and then the orientation will be randomized. This approach was first used to improve the extinction formula for randomly oriented prolate spheroids (Ref. 10). This work also underlines the fact that ignoring the deviated ray produces unacceptable errors for convex elongated oriented particles.

UNCLASSIFIED

18

## 4.1 Oriented Infinite Cylinders

The extended anomalous diffraction formula for oriented infinite cylinders is given by [1], except that the phase difference $\omega$ now takes into account the refraction of the central ray through the cylinder:

$$Q_{ad} = \pi \operatorname{Re}[\mathbf{H}_1(\omega) + i\mathbf{J}_1(\omega)] \qquad [30]$$

where $\omega$ is now given by

$$\omega = \psi x = 2x[(m^2 - \cos^2 \theta)^{1/2} - \sin \theta]. \qquad [31]$$

Using [21] and [23], the edge term for oriented infinite cylinders in the extended anomalous approximation is

$$
\begin{aligned}
\overline{Q}_{edge} &= \frac{c_0}{(x^{2/3} + x_{crit})\sin^{2/3}\theta} \\
x_{crit} &= \frac{3.6}{4|(m^2 - \cos^2\theta)^{1/2} - \sin\theta|}.
\end{aligned}
\qquad [32]
$$

Since the first maximum of the $\mathbf{H}_1(z)$ occurs at about $z = 3.6$, the above has $\rho_{max} = 3.6$.

To be complete, [31] for the standard anomalous approach is

$$\omega = \psi x = 2x(m-1)/\sin\theta. \qquad [33]$$

and the edge term for undeviated rays is [32] but now

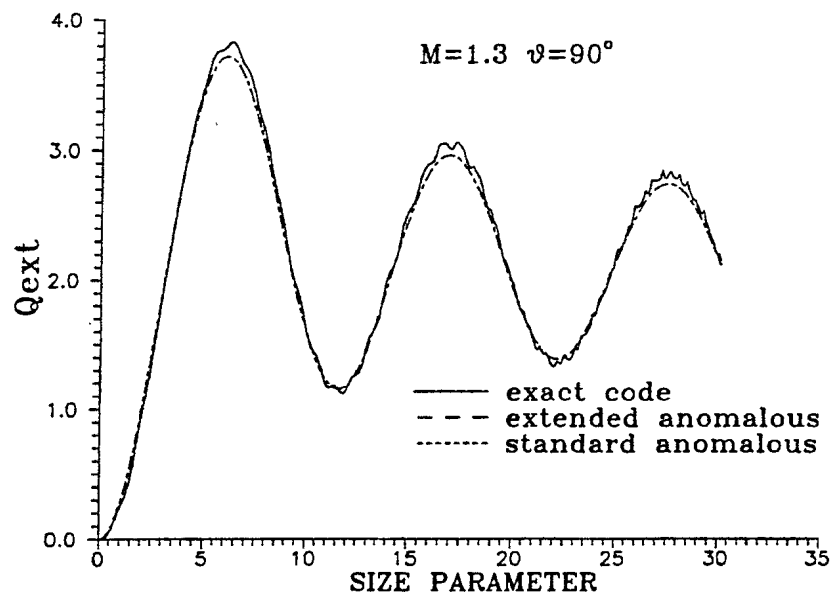$$x_{crit} = \frac{3.6\sin\theta}{4|m-1|} \qquad [34]$$

19



FIGURE 9 – Effect of extended anomalous diffraction on $Q_{ext}$. The index is 1.3 and orientation angle is 90°.

The effects of this extension on the extinction for a particular orientation can be dramatic, as shown in the next sequence of three figures. The orientation angle is decreased from 90° to 30°. For Fig. 9 there is no difference between the standard and extended anomalous diffraction approaches since there is no deviation of the central ray. For 60°, Fig. 10, the phase of the standard anomalous diffraction solution is clearly incorrect and this error accumulates at larger $x$. At 30°, Fig. 11, the situation worsens. This continues for smaller orientation angles.
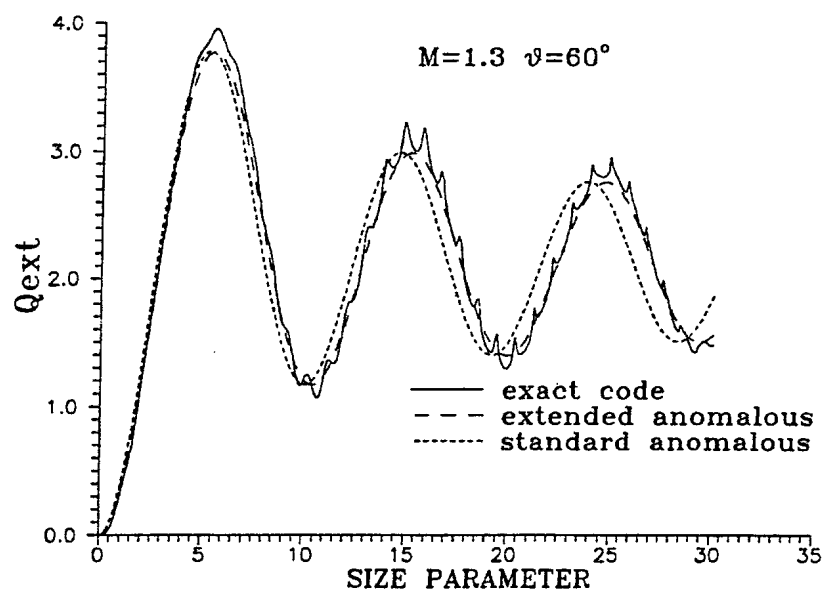
20



FIGURE 10 – Effect of extended anomalous diffraction on $Q_{ext}$. The index is 1.3 and orientation angle is 60°.



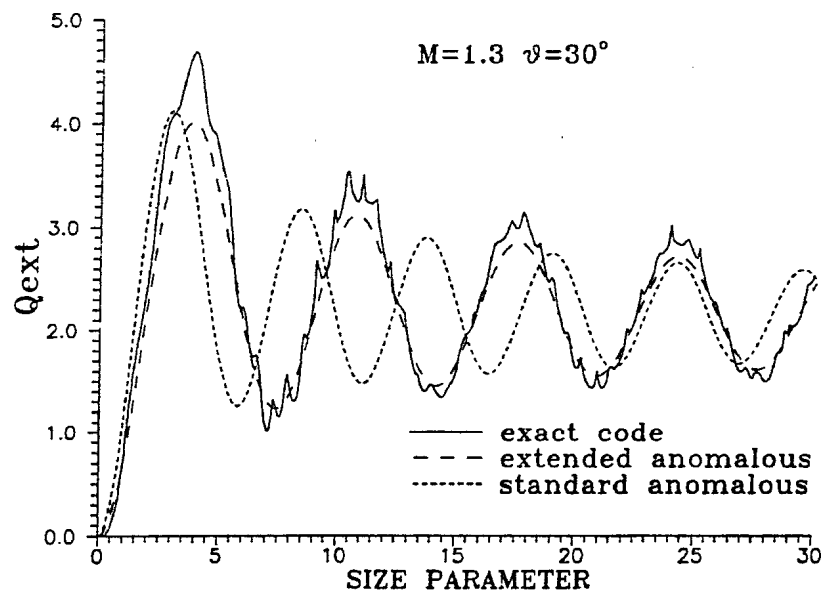FIGURE 11 – Effect of extended anomalous diffraction on $Q_{ext}$. The index is 1.3 and orientation angle is 30°.

## 4.2 Random Orientation

In the angle averaged case, the effects demonstrated by Figs. 9-11 can still be seen. This is shown in Figs. 12 and 13 for $m = 1.3$ and $m = 1.8$, respectively. Taking account of the deviated ray improves both the shape and amplitude of the estimate $Q_{ext}$. This is more evident at the higher index.

Since the Jacobian, $\sin^2 \theta$, weights towards 90°, the effect of ray deviation is not as dramatic as in the oriented case. Additionally, the integral produced by the angle averaging does not have an exact analytic solution. An approximate analytic formula has been obtained (Refs. 13-14), but is considerably more complex than [27] and has an error comparable to the improvement. Hence, it is satisfactory to consider only undeviated rays in approximating $Q_{ext}$ for random orientations if a simple efficient formula is of paramount importance.
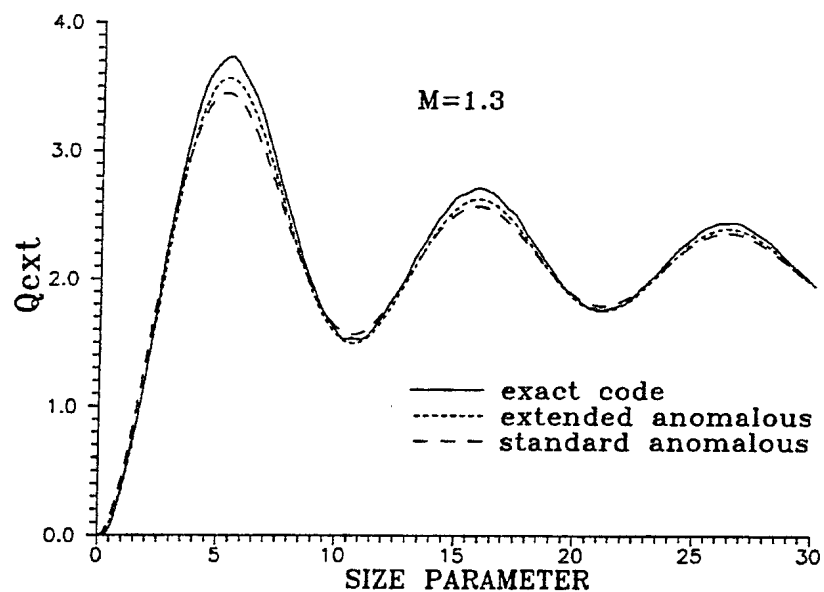
UNCLASSIFIED
22



FIGURE 12 – Effect of extended anomalous diffraction on $Q_{ext}$. The index is 1.3, random orientation.
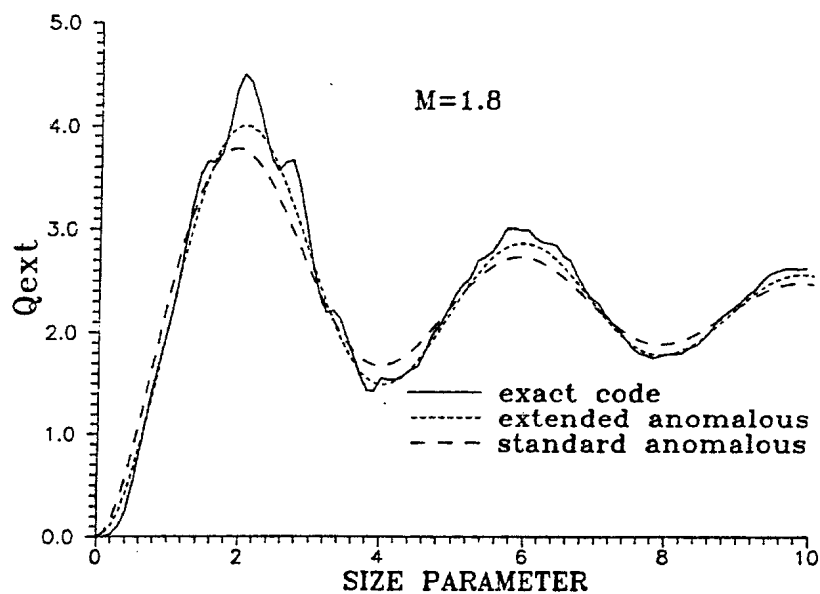


FIGURE 13 – Effect of extended anomalous diffraction on $Q_{ext}$. The index is 1.8, random orientation.

23

## 5.0   ELLIPTIC INFINITE CYLINDERS: AN EXTENSION

The power of the anomalous diffraction approach can be extended in a straightforward manner to infinite cylinders of elliptical cross sections. Since the extended anomalous diffraction generally leads to complicated expressions (Ref. 1), we will present only formula for the standard anomalous diffraction. We will first set up the formalism for the oriented case and then do the angle orientation.

### 5.1   Oriented Case

Let the infinite axis of the elliptic cylinder be oriented at an angle $\theta$ with respect to the direction of the incident radiation, as was the case for the circular cylinders. Take a cross section normal to the infinite axis of the cylinder. Let $\phi$ be the angle between the semi-major axis of the elliptical cross section of the cylinder and the plane defined by the direction of the incident radiation and the infinite axis of the cylinder. Let $p$ be the projection operator of this elliptical cross section onto the shadow plane (Ref. 3). Then,

$$p = \sqrt{\cos^2 \phi + r^2 \sin^2 \phi} \qquad [35]$$

where $r$ is the ratio of the semi-major axis size parameter $a$ to the semi-minor axis size parameter $b$ of the elliptic cross section. The anomalous diffraction expression $Q_{ad}$ for an infinite elliptical cylinder oriented at angles $\theta$ and $\phi$ is

$$Q_{ad} = \pi \mathrm{Re}[\mathrm{H}_1(\alpha) + i\mathrm{J}_1(\alpha)] \qquad [36]$$

24

where $\alpha$ is given by

$$\alpha = \frac{2(m-1)rb}{p \sin \theta}, \qquad [37]$$

Thus $Q_{ad}$ is the same as for the circular cylinder but with $x$ replaced by $rb/p$. The edge term is simply derived to be

$$Q_{edge} = \frac{c_0}{p^2} \left( \frac{r}{b \sin \theta} \right)^{2/3}. \qquad [38]$$

These equations allow us to study the randomly oriented case.

## 5.2    Random Orientation

The angle averaging must be done over two angles, $\theta$ and $\phi$. It is evident that the averaging over $\theta$ will give [27] with $\rho \to 2(n-1)rb/(p \sin \theta)$, $x \to rb/p$ and

$$\overline{Q}_{edge} = \frac{1.159595 \, c_0 \, r^{2/3}}{p^2[b^{2/3} + \pi/(4|m-1|)]}. \qquad [39]$$

This leaves the angle averaging over $\phi$ to be performed. An analytic expression can be found, but is complicated. However, it can be numerically integrated or approximated in various limits. The latter will be discussed in the next section.

Figures 14 and 15 are computations of the extinction efficiency predicted by standard anomalous diffraction plus edge term for randomly oriented elliptic cylinders. Figure 14 compares the results between a circular cylinder and an elliptic cylinder with $r = 2$. Figure 15 is the same, but $r = 3$ for the elliptic cylinder. Note that the peaks are shifted towards smaller $b$ and the amplitudes are reduced with increasing $r$. Most of the peak shift occurs between $r = 1$ and $r = 2$.
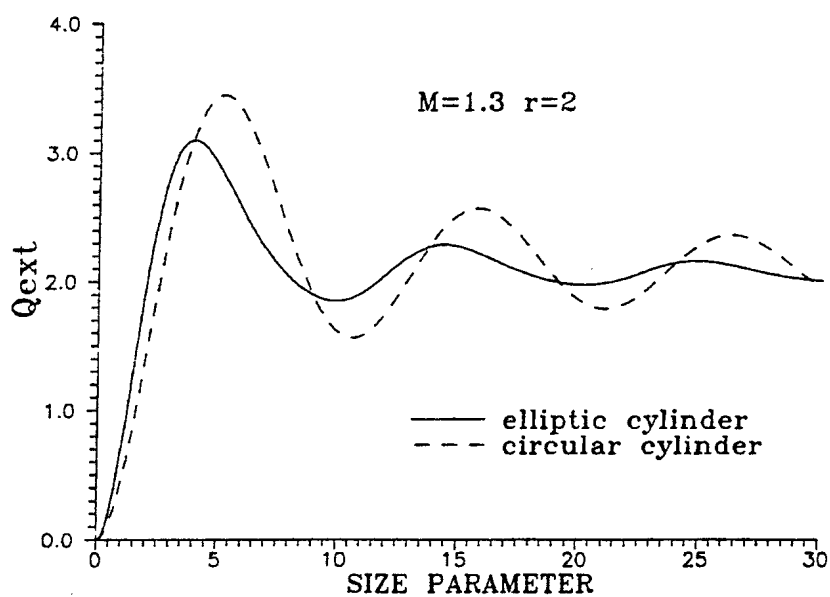
25



FIGURE 14 – Comparison between randomly oriented circular cylinders and elliptic cylinders. The index is 1.3 and $r = 2$.
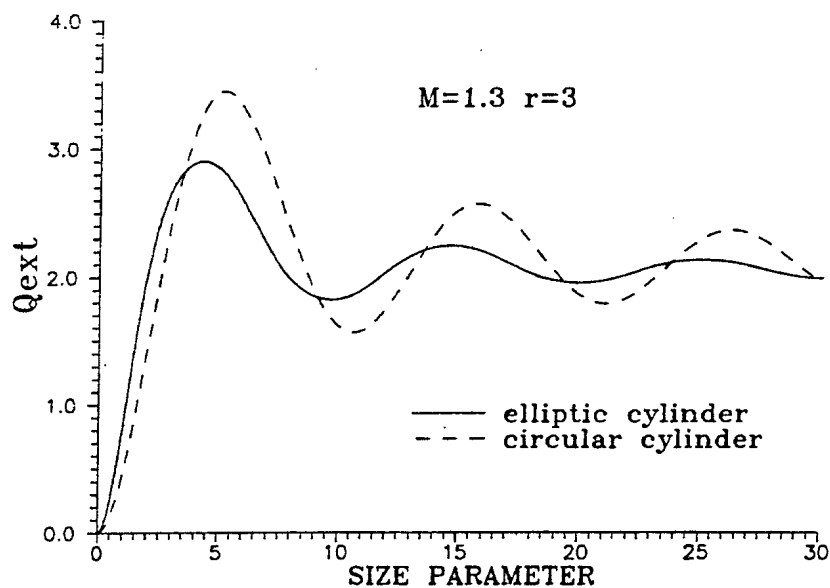


FIGURE 15 – Comparison between randomly oriented circular cylinders and elliptic cylinders. The index is 1.3 and $r = 3$.

26

## 5.3  Approximations

If we make the same substitution, as was done in the previous section but into the asymptotic form [28] and then perform an approximate angle averaging over the first terms only one obtains a simple and reasonably accurate expression for the extinction efficiency. Thus the completely angle averaged extinction efficiency, $< Q_{ad} >$, is approximately

$$< Q_{ad} > \approx 2 - \frac{4}{E(\epsilon^2)} \int_0^{\pi/2} \frac{\cos(\alpha r/p)}{\alpha r} p^2 \, d\phi \qquad [40]$$

where $E(\epsilon^2)$ is the complete elliptic integral of the second kind, $\epsilon^2 = 1 - 1/r^2$ is the square of the eccentricity and $\alpha = 2(n-1)b$.

The integral in the second term of [40] must be approximated. By rewritting $p = \sqrt{(\cos^2(\phi) + r^2 \sin^2(\phi))}$ as $r\sqrt{1 - \epsilon^2 \cos^2(\phi)} = rp'$ we can expand $1/p$ in terms of $\epsilon^2$, which is always between 0 and 1 and hence small. Thus

$$\frac{1}{p} \approx \frac{1}{r}[1 + f(\epsilon^2)\cos^2(\phi)]. \qquad [41]$$

If the Taylor expansion is used then $f(\epsilon^2) = \epsilon^2/2$. This function, as will be shown later, can be better optimized.

Putting [41] into the integral in [40], we get

$$\int_0^{\pi/2} \frac{\cos(\alpha r/p)}{\alpha r} p^2 \, d\phi \approx \frac{1}{\alpha} \int_0^{\pi/2} \cos[\alpha(1 + f(\epsilon^2)\cos^2(\phi))][1 - \epsilon^2 \cos^2(\phi)] \, d\phi. \qquad [42]$$

After some significant algebra the evaluation of [42] requires performing the follow-

27

ing integrals:

$$I_1 = \int_0^{\pi/2} \cos(2\beta \cos^2(\phi)) \, d\phi = \frac{\pi}{2} \cos(\beta) \, J_0(\beta) \qquad [43]$$

$$I_2 = \int_0^{\pi/2} \sin(2\beta \cos^2(\phi)) \, d\phi = \frac{\pi}{2} \sin(\beta) \, J_0(\beta) \qquad [44]$$

$$I_3 = \int_0^{\pi/2} \cos(2\beta \cos^2(\phi)) \cos^2(\phi) \, d\phi = \frac{\pi}{4} \, {}_2F_3 \left[ \begin{array}{c} 3/4, 5/4 \\ 1/2, 1, 3/2 \end{array} \middle| -\beta^2 \right].$$

$$= \frac{\pi}{4} [\cos(\beta) \, J_0(\beta) - \sin(\beta) \, J_1(\beta)] \qquad [45]$$

$$I_4 = \int_0^{\pi/2} \sin(2\beta \cos^2(\phi)) \cos^2(\phi) \, d\phi = \frac{3\pi\beta}{8} \, {}_2F_3 \left[ \begin{array}{c} 5/4, 7/4 \\ 3/2, 3/2, 2 \end{array} \middle| -\beta^2 \right]$$

$$= \frac{\pi}{4} [\sin(\beta) \, J_0(\beta) + \cos(\beta) \, J_1(\beta)] \qquad [46]$$

In the above, $I_1$ to $I_4$ can be obtained by using Mathematica V.2.2. The reduction of the two ${}_2F_3$ hypergeometric functions in $I_3$ and $I_4$ requires breaking them into their even and odd parts (MacRobert's theorem) and then using the reduction tables (Ref. 8).

Putting these results into [40], we finally obtain

$$< Q_{ad} > \approx 2 - \frac{2\pi}{E(\epsilon^2)} \left\{ \frac{\cos(\alpha)}{\alpha} \left[ \left(1 - \frac{\epsilon^2}{2}\right) \cos(\beta) J_0(\beta) + \frac{\epsilon^2}{2} \sin(\beta) J_1(\beta) \right] \right. \qquad [47]$$

$$\left. - \frac{\sin(\alpha)}{\alpha} \left[ \left(1 - \frac{\epsilon^2}{2}\right) \sin(\beta) J_0(\beta) - \frac{\epsilon^2}{2} \cos(\beta) J_1(\beta) \right] \right\} \qquad [48]$$

where $\beta = \alpha f(\epsilon^2)$.

There remains to determine an optimal form for $f(\epsilon^2)$. A simple but effective approach is to minimize the least-square error, $\mathcal{E}$, of $1/p$ or $1/p'$ and [41] i.e:

$$\mathcal{E} = \text{Min} \left\{ \int_0^{\pi/2} \left[ (1 + f(\epsilon^2) \cos^2(\phi))(p')^2 - p' \right]^2 \, d\phi \right\}. \qquad [49]$$

28

Thus

$$\frac{\partial \mathcal{E}}{\partial f} = 2 \int_0^{\pi/2} \left[ (1 + f(\epsilon^2)\cos^2(\phi))(p')^2 - p' \right] \cos^2(\phi)\,(p')^2\,d\phi = 0. \qquad [50]$$

Solving for $f$ we get

$$f(\epsilon^2) = \left[ \int_0^{\pi/2} (p')^3 \cos^2(\phi)\,d\phi - \int_0^{\pi/2} (p')^4 \cos^2(\phi)\,d\phi \right] / \int_0^{\pi/2} (p')^4 \cos^4(\phi)\,d\phi \equiv [I_5 - I_6]/I_7$$

$$[51]$$

The above three integrals $I_5$ to $I_7$ can be solved again by using Mathematica and the Gauss

contiguity relations (Ref.5). Thus

$$I_5 = \int_0^{\pi/2} (p')^3 \cos^2(\phi)\,d\phi = \frac{\pi}{4}\,{}_2F_1\left[ \begin{matrix} -3/2, 3/2 \\ 2 \end{matrix} \middle| \epsilon^2 \right]$$

$$= \frac{1}{15\epsilon^2}[(3 - 7\epsilon^2 + 4\epsilon^4)K(\epsilon^2) - (3 - 13\epsilon^2 + 8\epsilon^4)E(\epsilon^2)]$$

$$\approx \frac{\pi}{2(4 - \epsilon^2)}\left[ 2 + \left( \frac{4}{5\pi} - 3 \right)\epsilon^2 + \epsilon^4 \right] \qquad [52]$$

$$I_6 = \int_0^{\pi/2} (p')^4 \cos^2(\phi)\,d\phi$$

$$= \frac{\pi}{8}\left[ 2 - 3\epsilon^2 + \frac{5}{4}\epsilon^4 \right] \qquad [53]$$

$$I_7 = \int_0^{\pi/2} (p')^4 \cos^4(\phi)\,d\phi$$

$$= \frac{\pi}{16}\left[ 3 - 5\epsilon^2 + \frac{35}{16}\epsilon^4 \right]. \qquad [54]$$

In the above $K(\epsilon^2)$ is the complete elliptic integral of the first kind. The approximation in

[52] is a rational approximation with matched asymptotes to simplify the computation, if

required. This gives a rational form for $f(\epsilon^2)$ that is very close to the Taylor solution for

$\epsilon \to 0$. It is nearly a factor of 2 larger than the Taylor, however, when $\epsilon \to 1$ and hence it

is where one expects the greatest improvement in $< Q_{ad} >$.

A second approximation, that is good for small $\epsilon^2$, can be obtained by a Taylor expansion of $< Q_{ad} >$ about $\epsilon^2 = 0$, i.e.

$$< Q_{ad}(\epsilon^2) >=< Q_{ad}(0) > +\epsilon^2 \left. \frac{\partial < Q_{ad}(\epsilon^2) >}{\partial \epsilon^2} \right|_{\epsilon^2=0} + \dots . \qquad [55]$$

This expansion will be not only restricted to small $\epsilon^2$ but also small $b$ since the phase information in $< Q_{ad} >$ is also being approximated. With some algebraic manipulation the second term on the right-hand side becomes

$$\left. \frac{\partial < Q_{ad}(\epsilon^2) >}{\partial \epsilon^2} \right|_{\epsilon^2=0} = \frac{\alpha^2}{3} - \frac{\pi \alpha^3}{16} \left\{ {}_1F_2 \left[ \begin{matrix} 1/2 \\ 2,3 \end{matrix} \Big| -\frac{\alpha^2}{4} \right] - \frac{\alpha^2}{48} {}_1F_2 \left[ \begin{matrix} 3/2 \\ 3,4 \end{matrix} \Big| -\frac{\alpha^2}{4} \right] \right\} + \frac{1}{4} < Q_{ad}(0) >$$

$$[56]$$

Hence, with additional work, the approximation to $< Q_{ad}(\epsilon^2) >$ for small $\epsilon^2$ and $b$ becomes

$$
\begin{aligned}
< Q_{ad}(\epsilon^2) > &\approx \left( 1 + \frac{\epsilon^2}{2} \right) < Q_{ad}(0) > - \frac{\pi \epsilon^2 \alpha}{2} J_1^2 \left( \frac{\alpha}{2} \right) \\
&= \left( 1 + \frac{\epsilon^2}{2} \right) \frac{4\alpha^2}{3} \left\{ 1 - \frac{\pi \alpha}{4} \left[ J_0^2 \left( \frac{\alpha}{2} \right) - \frac{2}{\alpha} J_0 \left( \frac{\alpha}{2} \right) J_1 \left( \frac{\alpha}{2} \right) + \left( 1 - \frac{2}{\alpha^2} \right) J_1^2 \left( \frac{\alpha}{2} \right) \right] \right\} \\
&\qquad\qquad - \frac{\pi \epsilon^2 \alpha}{2} J_1^2 \left( \frac{\alpha}{2} \right) \qquad [57]
\end{aligned}
$$

An additional approximation can be obtained by taking a formal asymptotic expansion of [28] (Ref. 16). Following the formula (6.3.28) and (6.3.38) of (Ref. 16) we get

$$
\begin{aligned}
< Q_{ad} > \; &\asymp \; 2 - \frac{2}{\alpha E(\epsilon^2)} \sqrt{\frac{2\pi}{\epsilon^2 \alpha}} \left[ (1 - \epsilon^2)^{7/4} \cos \left( \frac{\alpha}{\sqrt{1 - \epsilon^2}} - \frac{\pi}{4} \right) + \cos \left( \alpha + \frac{\pi}{4} \right) \right] + \\
&\quad \frac{1}{\alpha^2 E(\epsilon^2)} \left\{ (2 - \epsilon^2) E(\epsilon^2) - \frac{1 - \epsilon^2}{2} K(\epsilon^2) - \right. \\
&\quad \left. 3 \sqrt{\frac{2\pi}{\epsilon^2 \alpha}} \left[ (1 - \epsilon^2)^{9/4} \sin \left( \frac{\alpha}{\sqrt{1 - \epsilon^2}} - \frac{\pi}{4} \right) + \sin \left( \alpha + \frac{\pi}{4} \right) \right] \right\} \qquad [58]
\end{aligned}
$$

This formula is asymptotic in $\alpha$ and $\epsilon$. It is clear that, as $\epsilon$ goes to 0, [58] does not go to the asymptotic circular cylinder formula [28]. This can be easily corrected by multiplying
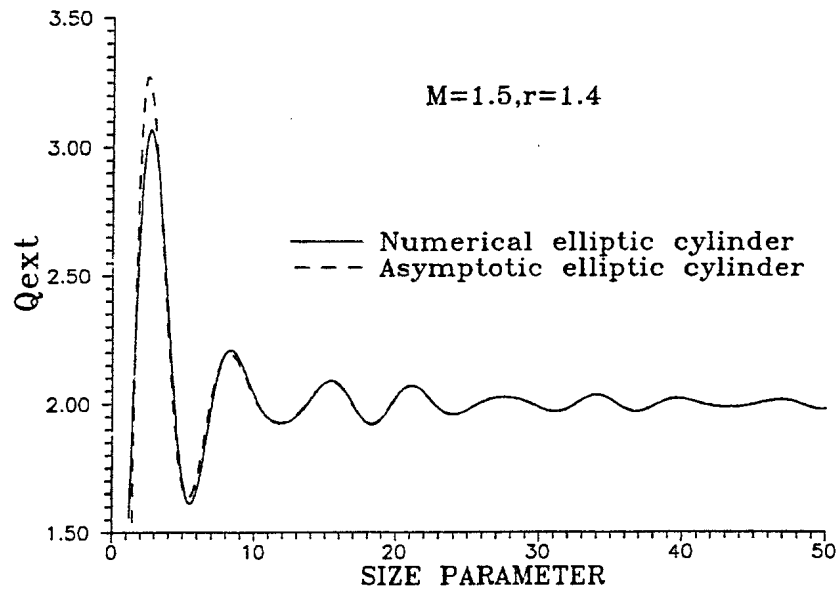
30



FIGURE 16 – Comparison between numerically integrated $< Q_{ad} >$ and [58]. The index is 1.5 and $r = 1.4$. (Note that $\alpha = b$).

the relevant terms in [58] by $1 - e^{-\sqrt{\pi \epsilon^2 \alpha}/2}$. The result is

$$
< Q_{ad} > \approx
$$

$$
2 + \frac{1}{\alpha^2 E(\epsilon^2)} \left[ (2 - \epsilon^2) E(\epsilon^2) - \frac{1 - \epsilon^2}{2} K(\epsilon^2) \right] -
$$

$$
\left( 1 - e^{-\sqrt{\pi \epsilon^2 \alpha}/2} \right) \frac{1}{\alpha E(\epsilon^2)} \sqrt{\frac{2\pi}{\epsilon^2 \alpha}} \left\{ 2 \left[ (1 - \epsilon^2)^{7/4} \cos \left( \frac{\alpha}{\sqrt{1 - \epsilon^2}} - \frac{\pi}{4} \right) + \cos \left( \alpha + \frac{\pi}{4} \right) \right] + \right.
$$

$$
\left. \frac{3}{\alpha} \left[ (1 - \epsilon^2)^{9/4} \sin \left( \frac{\alpha}{\sqrt{1 - \epsilon^2}} - \frac{\pi}{4} \right) + \sin \left( \alpha + \frac{\pi}{4} \right) \right] \right\} \qquad [59]
$$

This formula is now asymptotic in $\alpha$, for any $\epsilon$.

Figure 16 is a comparison between the numerically calculated $< Q_{ad} >$ and [59]. The numerical integration was carried out by using a 256-point Gaussian quadrature. It is surprising that such a simple expression as [59] can capture all of the subtle features of the oscillations.

31

This formula makes it obvious that the extinction peaks for large aspect cylinders occur near $\pi(n - 1/4)$. This formula forms an excellent backbone to $< Q_{ext} >$. All that remains is to add the effects of absorption and the edge terms in a manner similar to that done for circular cylinders. Hence, the addition of absorption is performed as in [18]. All that is required is the following simple integration to obtain the averaged absorption length $\lambda$:

$$
\begin{aligned}
\lambda &= \frac{1}{E(\epsilon^2)} \int_0^{\pi/2} \left(\frac{2kb}{p'}\right) p' \, d\phi \\
&= \frac{\pi kb}{E(\epsilon^2)}
\end{aligned}
\tag{60}
$$

The edge term also requires just a simple integration. It is set up by using [39] and changing the $x_{crit}$, $\pi/(4|m - 1|)$) by the semi-empirical form $\pi(1 - \epsilon^2/4)/(4|m - 1|b)$. See the disscusion concerning [23].

$$
\begin{aligned}
< Q_{edge} > &= \frac{1.159595 \, c_0}{r^{4/3}[b^{2/3} + \pi(1 - \epsilon^2/4)/(4|m - 1|)]E(\epsilon^2)} \int_0^{\pi/2} \left(\frac{1}{(p')^2}\right) p' \, d\phi \\
&= \frac{1.159595 \, c_0}{r^{4/3}[b^{2/3} + \pi(1 - \epsilon^2/4)/(4|m - 1|)]} \frac{K(\epsilon^2)}{E(\epsilon^2)}
\end{aligned}
\tag{61}
$$

Thus, the asymptotic formula for $< Q_{ext} >$ is

$$
< Q_{ext} > \asymp \left[2 - e^{-\lambda}(< Q_{ad} > -2)\right] \left(1 - e^{-<Q_{edge}>/2}\right)
\tag{62}
$$

Unfortunately, the accuracy of the above formula cannot at present be determined since there are no known results for randomly oriented elliptic cylinders. The results to date are for a particular orientation only (see Ref. 17 and references therein).

32

## 6.0   CONCLUSIONS AND LIMITATIONS

We have presented an analytic approximation to $Q_{ext}$ for oriented and randomly oriented infinite cylinders of circular cross section. In addition, a formula requiring only one numerical integration is given for randomly oriented infinite cylinders of elliptic cross section. Various asymptotic expressions for these formulae are also developed.

The large size regime is modelled by anomalous diffraction plus 'edge' or Fock terms as in Ref. 1. The small particle size limit, although roughly modelled, is not treated extensively since the resulting formulae would be too complex. Furthermore, at least in the case of circular infinite cylinders, the exact code is efficient in this regime.

An extension to the anomalous diffraction approach, similar to that in Ref. 1, is also developed for the case of circular cylinders. This demonstrates that this extended anomalous diffraction is significant only when the cylinders are oriented.

The circular cylinder formula gives good results with little loss in accuracy for medium to large size parameters for $n \geq 1$ and $0 \leq k \leq 3$ and, for elliptic cylinders, for modest aspect ratios ($r \leq 4$). Typical errors of about 5% or less are encountered in the circular cylinder case. The errors observed have the same behaviour as previous seen for randomly oriented spheroids (Ref. 1). Errors for the elliptic cylinder cannot be determined at this date since there are no known exact results (Ref.17). However, there is no physical reason we know of that would make the errors in the formulae behave differently for elliptical

33

cylinders than that of either the circular cylinders or spheroids.

If high precision is not required, the circular cylinder formula is far more economical in computer time than the exact random infinite cylinder code. This is even more true when considering elliptical cylinders or polydispersions. Taking account of both the range of demonstrated validity and the accuracy, the circular cylinder formula is superior to all other approximations known by the authors.

An even simpler form for large optical sizes is also derived for both the circular and elliptic cylinders which are analogues of Van de Hulst's famous formula for spheres. This allows for the simple determination of the maxima and minima of the extinction.

The results of this work demonstrates, once again, the effectiveness of the combined approaches of anomalous diffraction and edge effect terms in modelling the extinction from smooth convex bodies. This is a positive signal towards further work on other shapes and scattering properties to fully cover the broad spectrum of natural and artifical scatterers.

34

## 7.0 REFERENCES

1. Evans, B.T.N. and Fournier, G.R., "Analytic Approximation to Randomly Oriented Spheroid Extinction", Applied Optics, Vol. 33, No. 24, p. 5796, 1994.

2. Evans, B.T.N., "An Interactive Program for Estimating Extinction and Scattering Properties of Most Particulate Clouds", MRL R-1123/88, June, 1988, UNCLASSIFIED.

3. Van de Hulst, H.C., "Light Scattering by Small Particles", 1st Edition, John Wiley & Sons, New York, 1957.

4. Stephens, G.L., "Scattering of Plane Waves by Soft Obstacles: Anomalous Diffraction Theory for Circular Cylinders", Applied Optics, Vol. 23, No. 6, p. 954, 1984.

5. Abramowitz, M., Stegun, I.A., Eds., "Handbook of Mathematical Functions", Eighth Dover Edition, New York, 1972.

6. Erdélyi, A., Magnus, W., Oberhettinger, F. and Tricomi, F.G., "Tables of Integral Transforms", Vol. II, McGraw-Hill, New York, 1954.

7. Luke, Y.L., "The Special Functions and Their Approximations", Vols. I and II, Academic Press, New York, 1969.

8. Prudnikov, A.P., Brychkov, Yu. A., Marichev, O.I.,"Tables of Integrals and Series Vol. 3: More Special Functions", Gordon and Breach, London, 1990.

9. Jones, D.S., "High-Frequency Scattering of Electromagnetic Waves," Proc. R. Soc. London, Ser. A 240, p. 206, 1957.

10. Fournier, G.R. and Evans, B.T.N., "Approximation to Extinction Efficiency for Randomly Oriented Spheroids", Applied Optics, Vol. 30, No. 15, p. 2042, 1991.

11. Nussenzveig, H.M. and Wiscombe, W.J., "Efficiency Factors in Mie Scattering", Phys. Rev. Lett., 45, p. 1490, 1980.

12. Beckmann, V.P. and Franz, W., "Berechnung der Streuquerschnitte von Kugel und Zylinder unter Anwendung einer modifizierten Watson-Transformation, ", Z. Naturforschg., 12a, p. 533, 1957.

UNCLASSIFIED
35

13. Evans, B.T.N. and Fournier, G.R., "A Procedure for Obtaining an Algebraic Approximation to Certain Integrals", DREV R-4653/91, August, 1991, UNCLASSIFIED

14. Evans, B.T.N. and Fournier, G.R., "Algebraic Approximation to Some Integrals in Optics", J. Phys. A: Math. Gen. 26, p. 647, 1993.

15. Wolfram, S., "Mathematica: A System for Doing Mathematics by Computer", Addison-Wesley, New York, 1989.

16. Bleistein, N., and Handelsman, R.A., "Asymptotic Expansions of Integrals", Dover Publications, New York, 1986.

17. Kim, C.S., and Yeh, C., "Scattering of an Obliquely Incident Wave by a Multilayered Elliptical Lossy Dielectric Cylinder", Radio Science, Vol. 26, No. 5, pp. 1165-1176, 1991.

UNCLASSIFIED
36

## INTERNAL DISTRIBUTION

### DREV R-9425

1 &ndash; Deputy Director General
1 &ndash; Director Electro-optics and Surveillance Division
1 &ndash; Director Weapon Systems Division
6 &ndash; Document Library
1 &ndash; Dr. B.T.N. Evans (author)
1 &ndash; Dr. G.R. Fournier (author)
1 &ndash; Dr. P. Pace
1 &ndash; Dr. L. Bissonnette
1 &ndash; Mr. D. Hutt
1 &ndash; Mr. G. Roy

UNCLASSIFIED
37

## EXTERNAL DISTRIBUTION

### DREV R-9425

2 &ndash; DSIS
1 &ndash; CRAD
1 &ndash; DRDL
1 &ndash; DRDM
1 &ndash; DMCS
1 &ndash; Mr. R. Kluchert, DLOR, NDHQ

1 &ndash; Dr. W.G. Tam
Senior Project Manager
Industrial Research Assistance Program
Laboratory Network
National Research Council
Ottawa, Ontario
K1A 0R6

1 &ndash; Dr. A.I. Carswell
Dept. of Physics
York University
4700 Keele Street
North York, Ontario
M3J 1P3

1 &ndash; Dr. T. Platt
Biological Oceanography Division
Department of Fisheries and Oceans
Bedford Institute of Oceanography
P.O. Box 1006
Dartmouth, N.S. B2Y 4A2

1 &ndash; Dr. D. K. Cohoon
West Chester University
Dept. of Mathematics and Computer Science
West Chester, PA, 19383
USA

UNCLASSIFIED
38


## EXTERNAL DISTRIBUTION (contd)


### DREV R–9425


1  –  Dr. B.P. Curry
NPB Test Stand
Engineering Physics
Argonne National Lab.
9700 South Cass Ave., EP/207
Argonne, IL, 60439-4841
USA


1  –  Dr. J. Embury
Chemical Research, Development and Engineering Center
SMCRR-RSP-B
Aberdeen Proving Ground, MD, 21010-5423
USA


1  –  Dr. P. Barber
Clarkson College of Technology
Dept. of Electrical & Computer Engineering
Potsdam, NY, 13676
USA


1  –  Dr. M. Lax
City College of New York
Physics Dept.
New York, NY, 10031
USA


1  –  Dr. R.T. Wang
ISST- Space Astronomy Lab.
1810 NW 6th st.
Gainesville, FL, 32609
USA


1  –  Dr. G. Kunz
Physics Laboratory TNO
P.O. Box 9 68 64
2509 The Hague
The Netherlands

UNCLASSIFIED
39

EXTERNAL DISTRIBUTION (contd)

DREV R-9425

1 — Dr. C.M.P. Platt
CSIRO
Division of Atmospheric Research
Private Bag No. 1, Mordialloc, Vic 3195
Australia

1 — Dr. Mayo Greenburg
Laboratory Astrophysics
Leiden University
Postbus 9504
2300 RA Leiden
The Netherlands

## DOCUMENT CONTROL DATA

| 1. ORIGINATOR (name and address)<br><br>Defence Research Establishment, Valcartier<br>2459 Pie XI Blvd. North<br>P.O. Box 8800<br>Courcelette, Qc<br>G0A 1R0 | 2. SECURITY CLASSIFICATION<br>(Including special warning terms if applicable)<br><br>UNCLASSIFIED |
|---|---|

| 3. TITLE (Its classification should be indicated by the appropriate abbreviation (S,C, or U.)<br><br>Algebraic Approximations to Extinction from Randomly Oriented Circular and Elliptical Cylinders |
|---|

| 4. AUTHORS (Last name, first name, middle initial. If military, show rank, e.g. Doe, Maj. John E.)<br><br>Fournier, G.R. and Evans, B.T.N. |
|---|

| 5. DATE OF PUBLICATION (month and year)<br><br>1995 | 6a. NO. OF PAGES<br><br>27 | 6b. NO. OF REFERENCES<br><br>14 |
|---|---|---|

| 7. DESCRIPTIVE NOTES (the category of the document, e.g. report, memorandum, etc). Give the inclusive dates when a specific reporting period is covered.)<br><br>Report |
|---|

| 8. SPONSOR (name and address) |
|---|

| 9a. PROJECT OR GRANT NO. (Please specify whether project or grant.)<br><br>3733B-P312A-12A | 9b. CONTRACT NO.<br><br>N/A |
|---|---|

| 10a. ORIGINATOR'S DOCUMENT NUMBER<br><br>R. 9425 | 10b. OTHER DOCUMENT NOS.<br><br>N/A |
|---|---|

| 11. DOCUMENT AVAILABILITY (any limitations on further dissemination of the document, other than those imposed by security classification)<br><br>(X)  Unlimited distribution<br>(  )  Distribution limited to defence departments and defence contractors<br>(  )  Distribution limited to defence departments and Canadian defence contractors<br>(  )  Distribution limited to government departments and agencies<br>(  )  Distribution limited to defence departments<br>(  )  Other (please specify): |
|---|

| 12. DOCUMENT ANNOUNCEMENT (any limitation to the bibliographic announcement of this document. This will normally correspond to the Document Availability (11). However, where further distribution (beyond the audience specified in 11) is possible, a wider announcement audience may be selected.) |
|---|

13. ABSTRACT (a brief and factual summary of the document. It is highly desirable that the abstract of classified documents be unclassified. Each paragraph of the abstract shall begin with an indication of its security classification (unless the document itself is unclassified) represented as (S), (C), or (U).
It is not necessary to include here abstracts in both official languages unless the text is bilingual).

   Analytic approximations to the extinction efficiency, $Q_{ext}$, for oriented and randomly oriented circular infinite cylinders based on anomalous diffraction is given. The results are compared with the exact code. These results are further generalized to randomly oriented elliptical cylinders. Using the formulae, $Q_{ext}$ can be evaluated over $10^4$ times faster than with the exact code. This approximation is valid for complex refractive indices $m = n - ik$, where $1 \le n \le \infty$ and $0 \le k \le 3$, aspect ratios from 1 to 4 and modest to large particle sizes. The accuracy and limitations of this formula are discussed.

14. KEYWORDS, DESCRIPTORS or IDENTIFIERS (Technical terms or short phrases that characterize a document and could be helpful in cataloguing it. They should be selected so that no security classification is required. Identifiers, such as equipment model designation, trade name, military project code name, geographic location may also be included. If possible keywords should be selected from a published thesaurus, e.g. Thesaurus of Engineering and Scientific Terms (TEST) and that thesaurus identified. If it is not possible to select indexing terms which are Unclassified, the classification of each should be indicated as with the title.)

Extinction
Circular Infinite Cylinders
Elliptic Infinite Cylinders
Millimeter Waves

Requests for documents
should be sent to:

DIRECTOR SCIENTIFIC INFORMATION SERVICES
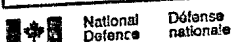Dept. of National Defence
Ottawa, Ontario
K1A 0K2
Tel: (613) 995-2971
Fax: (613) 996-0392

#152436

| NO. OF COPIES NOMBRE DE COPIES | COPY NO. COPIE Nº | INFORMATION SCIENTIST'S INITIALS INITIALES DE L'AGENT D'INFORMATION SCIENTIFIQUE |
|---|---|---|
| 1 | 1 | DAC |
| AQUISITION ROUTE FOURNI PAR ▶ | DBCU | |
| DATE ▶ | 30 Jun 95 | |
| DSIS ACCESSION NO. NUMÉRO DSIS ▶ | | |

DND 1158 (6-87)

National Defence  Défense nationale

PLEASE RETURN THIS DOCUMENT
TO THE FOLLOWING ADDRESS:
DIRECTOR
SCIENTIFIC INFORMATION SERVICES
NATIONAL DEFENCE
HEADQUARTERS
OTTAWA, ONT. - CANADA K1A 0K2

PRIÈRE DE RETOURNER CE DOCUMENT
À L'ADRESSE SUIVANTE:
DIRECTEUR
SERVICES D'INFORMATION SCIENTIFIQUES
QUARTIER GÉNÉRAL
DE LA DÉFENSE NATIONALE
OTTAWA, ONT. - CANADA K1A 0K2

Toute demande de document
doit être adressée à:

DIRECTEUR - SERVICES D'INFORMATION SCIENTIFIQUE
Ministère de la Défense nationale
Ottawa, Ontario
K1A 0K2

Téléphone: (613) 995-2971
Télécopieur: (613) 996-0392